

NANOSTRUCTURE OF RENEWABLE OXYGENATED FUELS PARTICULATE MATTER

Preechar Karin¹, Yutthana Songsaengchan¹, Songtam Laosuwan², Chinda Charoenphonphanich², Nuwong Chollacoop³, and Katsunori Hanamura⁴

¹International College, ²Faculty of Engineering, King Mongkut's Institute of Technology Ladkrabang, Ladkrabang, Bangkok, Thailand, e-mail:kkpreech@kmitl.ac.th

³National Metal and Materials Technology Center, National Science and Technology Development Agency, Bangkok, Thailand

⁴Department of Mechanical and Control Engineering, Tokyo Institute of Technology, Tokyo, Japan

Received Date: November 5, 2012

Abstract

This paper describes a part of an ongoing research project in diesel Particulate Matter (PM) reduction by using renewable oxygenated fuel. In order to achieve the particulate matter reduction, physical structure and aggregation behavior should be investigated for better understanding of designs and configurations of Diesel Particulate Filter (DPF). The nanostructures of diesel and biodiesel PMs were investigated by using a Scanning Electron Microscopy (SEM) and a Transmission Electron Microscopy (TEM) for better understanding. The primary size distributions as well as particulate structures were presented by means of scanning images. The average primary sizes of diesel and biodiesel fuels PMs are approximately 50-60 nm and 30-40 nm, respectively. The average carbon platelet sizes of diesel and biodiesel PMs are in the range of 0.5-3.0 nm. In addition, Thermo-gravimetric Analysis (TGA) was used to investigate chemical kinetics of particulate matter oxidation. The apparent activation energies of oxygenated hydrocarbon, diesel hydrocarbon and carbon oxidation are approximately 91 kJ/mol, 130 kJ/mol and 155 kJ/mol, respectively.

Keywords: Diesel engine, Diesel particulate filter, Oxygenated fuel, Particulate matter

Introduction

Among internal combustion engines, diesel engines have the highest thermal efficiency. However, particulate matters (PMs) must be removed from exhaust gases emitted from diesel engines to protect the environment and human health. Therefore, the regulation on the restriction of emission is increased.

Diesel particulate matters consist of a solid fraction (SOL) and a soluble organic fraction (SOF). Primary particles, composed of carbon and metallic ash, are coated with SOF and sulfate. The nanostructures of primary soot particles have been characterized using transmission electron microscopy (TEM) to understand them in details. The mean diameters of the primary and agglomerated particles are usually in the range of 20–80 nm and 80–300 nm, respectively. A primary soot particle has two distinct parts: an inner core and an outer shell. The inner core has a diameter of 10 nm and it is located at the central region of the primary particle. The composition of particles from a diesel engine may vary widely depending on the operating conditions and fuel composition [1–9].

Diesel particulate filters (DPFs) play an important role in particulate trapping and oxidation. A DPF is generally made of ceramic materials, such as cordierite or silicon carbide, consisting of many rectangular channels with alternate channels blocked using cement at each end. The exhaust gas is forced to flow through a channel wall having numerous micron-scale pores that trap the particle emissions. Furthermore, the collected

particulates must be oxidized to regenerate the DPF and reduce the back pressure on the diesel engine [10–17].

The problem of particle emissions from diesel engine should be reduced by development of high efficiency engine, after-treatment and pre-treatment technologies. The use of renewable oxygenated fuels is now a widespread means to reduce regulated pollutant emissions produced by internal combustion engines [9], as well as to reduce the greenhouse gas. However, particulate matter emitted from biodiesel must be investigated for better understanding to optimize the design of DPF configuration. The present research is to study the physical structure and oxidation behaviors of diesel and biodiesel particulate matters. The first objective is to investigate and compare the quantity, microstructure and nanostructure of diesel and biodiesel particulate matters by using DPF sample disc for particulate trapping, SEM and TEM for particulate structure investigation. The second objective is the study of diesel and biodiesel particulate matters oxidation kinetics by using Thermo-gravimetric analysis (TGA).

Experimental Setup

Particulate Matter Generator

Biodiesel which derived from palm-olein (biodiesel (B100) fuel of TIS 2313-2549) was used and compared with the results of commercial grade diesel (conventional diesel (B0) fuel of TIS 2155-2546). The carbon fraction of diesel and biodiesel are 82 and 78, respectively. Diesel and biodiesel diffusion flame particulate matters were generated by diesel and biodiesel lamps, as shown in Fig.1. The fuel consumption of each fuel was measured by weight loss respect to time for comparison in the view point of energy consumption. Particulate matters were introduced into the DPF samples by using the vacuum pump by controlling the constant gas flow rate and temperature base on the actual vehicle condition. The pressure drop between inlet and outlet of the DPF sample were measured in each trapping time by using manometer and in real time by pressure sensor.

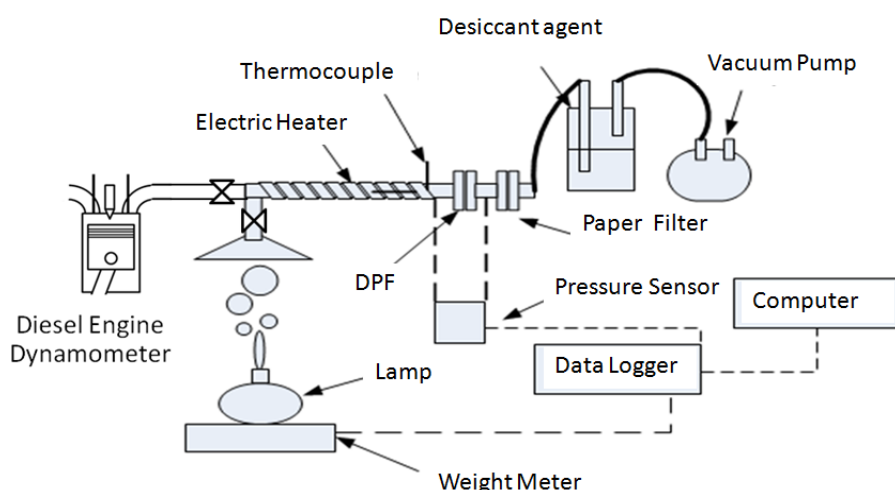


Figure 1. Experimental setup for particulate matter quantities investigation

On the other hand, a single cylinder, four strokes, direct injection diesel engine was also used in the soot generation process. The fuel injection pressure was 19.6 MPa and the engine speed was fixed at 2400 rpm without load on the engine dynamometer. The present research is focused on the effect of oxygenated fuel in particle emissions. Therefore,

no load condition is studied in this case for the first step even particulate matter size and unburned hydrocarbon content are strongly related to engine operating condition.

Particulate Matter Characterization Method

Nanostructures of single primary particle and carbon platelet structures were investigated by TEM image and post process by hand drawn images. Oxidation behaviors of isothermal and non-isothermal methods were investigated by TGA. Non-isothermal method was used to estimate apparent activation energy of each unburned hydrocarbon (oxygenated and fossil) under the condition of temperature increasing rate of 10°C per minute from 25°C to 800°C with 100% oxygen atmosphere. On the other hand, isothermal method was operated by temperature increasing rate of 10°C per minute from 25°C to 450°C to remove unburned hydrocarbon. Then, temperature was holding at 450°C for an hour. Similarly, each sample was tested under the condition of 500°C, 550°C and 600°C.

Chemical kinetics of particulate matter oxidation is studied by using Thermo-gravimetric analysis (TGA).



The chemical reaction rate in Equation 1 can calculate from the TGA curve based on the chemical kinetic in Equation 2

$$-\frac{d[C]}{dt} = -k[C]^n [O_2]^m \quad (2)$$

Where C is particulate matter mass, t is time, k is the rate constant of chemical reactions, m , n are the reaction orders. The dependence of the specific rate constant of chemical reactions k is expressed by Equation 3

$$k = Ae^{-E_a/RT} \quad (3)$$

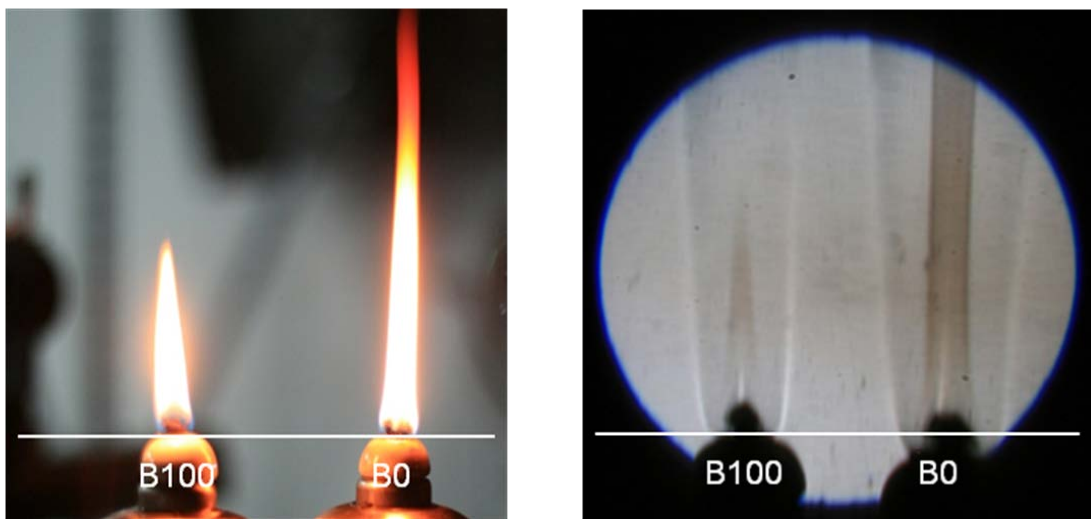
Where A is the frequency factor, E_a is the activation energy, R is the gas constant. The apparent activation energy can be calculated by Equation 4.

$$\ln \left[\frac{-1}{[C]^n} \frac{d[C]}{dt} \right] = -\frac{E}{RT} + (\ln A + m \ln [O_2]) \quad (4)$$

Results and Discussions

Particulate Matter Concentration

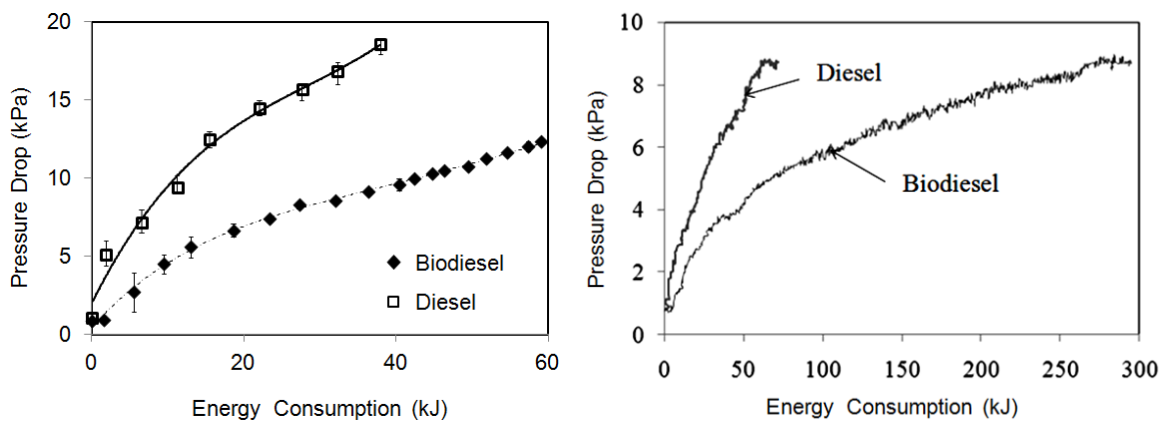
Figure 2 (a) shows diesel and biodiesel diffusion flames from optical image. The soot particle is formed in the fuel spray cores, in which the rich fuel is contained, whereas the fuel vapor is heated by mixing with hot burned gases in the flame regions. The particle is oxidized in the flame zone when it contacts with available oxygen, resulting in yellow luminous flame character. The length of biodiesel diffusion flame was shorter than that of diesel. Similarly, Figure 2 (b) shows diesel and biodiesel diffusion flames produced by Schlieren method. The center of biodiesel diffusion flame was lighter than that of diesel because oxygen atoms inside an oxygenated fuel molecule can promote the conditions which approach to the complete combustion.



(a) Conventional digital camera

(b) Schlieren method

Figure 2. Biodiesel (B100) and diesel (B0) diffusion flame by (a) optical digital camera and (b) Schlieren method images [18,19]

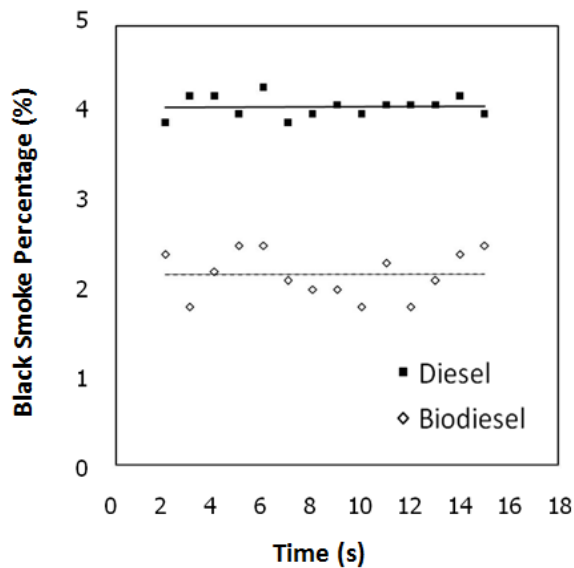


(a) Pressure Drop by Manometer

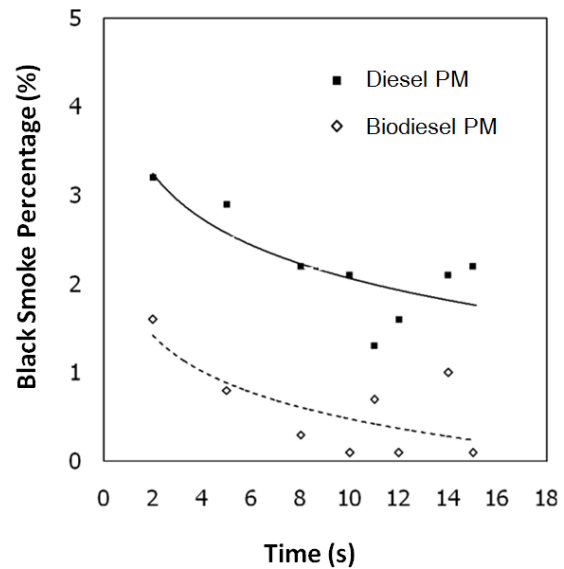
(b) Pressure Drop by Pressure Sensor

Figure 3. Lamp's diesel and biodiesel particulate matters concentrations by (a) manometer and [19,20] and (b) pressure sensor

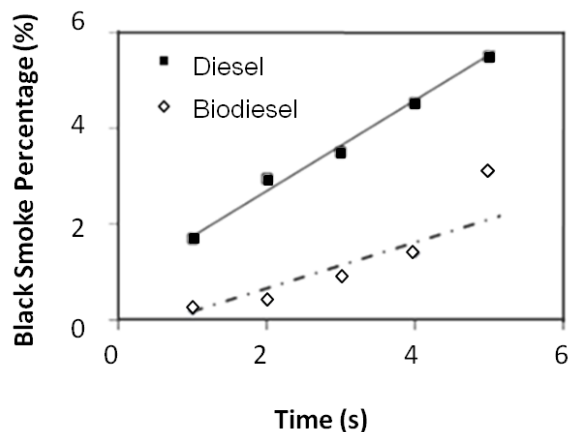
Figure 3 (a) shows the comparison of pressure drop between outlet and inlet of DPF disc sample with the size of $4.5 \times 4.5 \text{ cm}^2$. Samples were taken during the trapping process at the same energy consumption rate of diffusion flame. As indicated in this graph which obtained from measurement of manometer, diesel particulates have a higher pressure drop than biodiesel particulates at a given energy input. Pressure drop of DPF wall during diesel particulate matters trapping was approximately 2 times higher than that of biodiesel particulate matter. Therefore, the apparent amount of diesel particulate matter could be also assumed to be 2 times higher than that of biodiesel. However, the actual concentrations should be measured by using higher precision device in the next step. Figure 3 (b) shows the same trend of particulate matter trapping inside the DPF disc sample size of $6 \times 6 \text{ cm}^2$ and pressure drop was measured by pressure sensor.



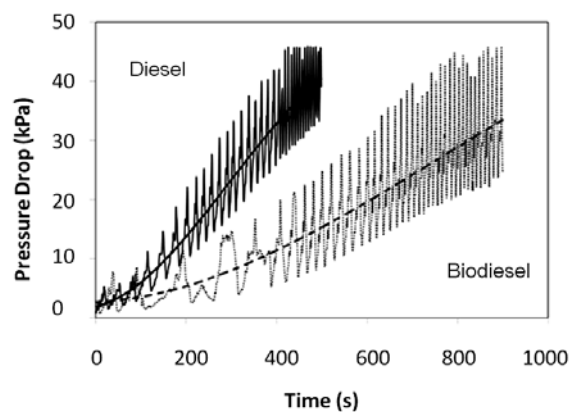
(a) Black smoke at DPF inlet



(b) Black smoke at DPF outlet



(c) Black smoke inside paper filter



(d) Pressure drop by pressure sensor

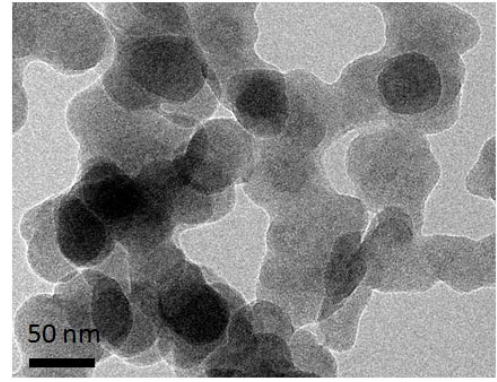
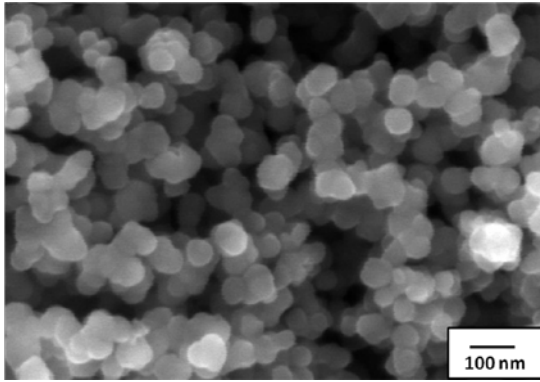
Figure 4. Engine's diesel and biodiesel particulate matters concentrations by smoke meter at (a) DPF inlet, (b) DPF outlet, (c) Inside paper filter [19,20] and by (d) Pressure sensor

In the same method, the remaining soot particle is emitted in the CI engine exhaust pipe. The paper filter was used to trap the emitted diesel and biodiesel soot particle at any time. Subsequently, smoke meter was applied to measure the concentration of trapped particulate on the paper filter by light emitting method. Figure 4 (a) and (b) show the percentage of black smoke of diesel and biodiesel at the inlet and outlet of DPF, respectively. The concentration of diesel black smoke is approximately two times higher than that of biodiesel. Figure 4 (c) shows the percentage of black smoke of diesel and biodiesel when the trapping period is varied. The result showed that the percentage of black smoke of diesel increased faster than that of biodiesel. In addition, it's also clearly observed that the pressure drop between inlet and outlet of DPF for diesel engine is approximately two times higher than that of biodiesel. Hence, diesel particulate formation was higher than biodiesel. This could be explained that more soot particulate was remained in diesel combustion than those of biodiesel. Because it contains oxygen molecule, biodiesel is readily oxidized with available oxygen in the flame zone. Consequently, particulate filter trapping duration of biodiesel fuel is longer than that of diesel fuel because of particulate concentration emitted from bio-oxygenated fuel combustion flame is lower than that of diesel combustion.

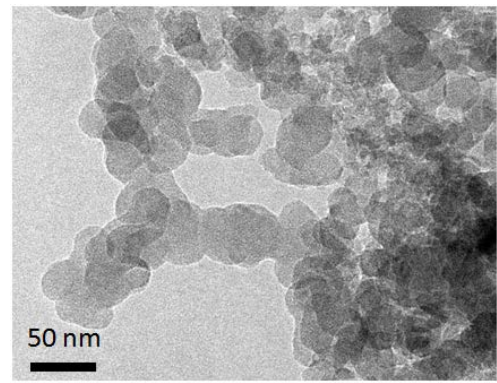
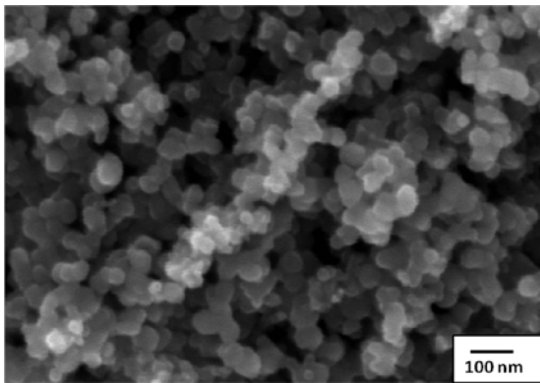
Microstructure of Particulate Matter

In this research, the particle image is taken to verify the diesel and biodiesel particle and carbon platelet sizes by micro- and nano- image. Figure 5 shows SEM images of ultrafine particle sizes from of (a) diesel lamp, (b) biodiesel lamp, (c) diesel engine and (d) biodiesel engine (left hand side). The image showed that the biodiesel particle sizes from both sources are slightly smaller than that of diesel particle. On the other hand, particle emitted from the lamp is a slightly smaller than that particle emitted from engine in both fuels. The single particle sizes from diesel and biodiesel diffusion flame are approximately 50-60 nm and 30-40 nm, respectively. However, it is difficult to measure primary size of engine particle by SEM image because the surface of particulate matter emitted from engine could be covered by much amount of unburned hydrocarbon. The TEM method was used to measure primary particle size from diesel and biodiesel fuel. Figures 5 (a), (b), (c) and (d) show particulate matter emitted from diesel lamp, biodiesel lamp, diesel engine and biodiesel engine (right hand side). The primary particle size is approximately 20-80 nm which is in the range of ultrafine particles (diameter size lower than 100 nm). However, the biodiesel particulate matter is a bit smaller than that of diesel particulate matter for both combustions.

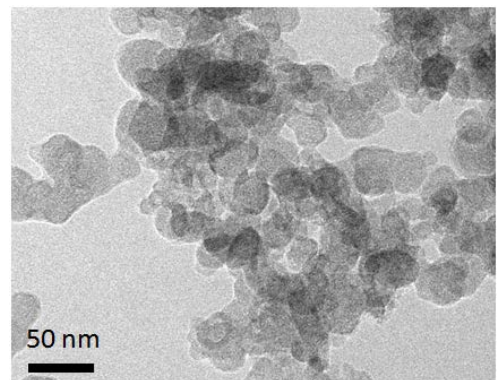
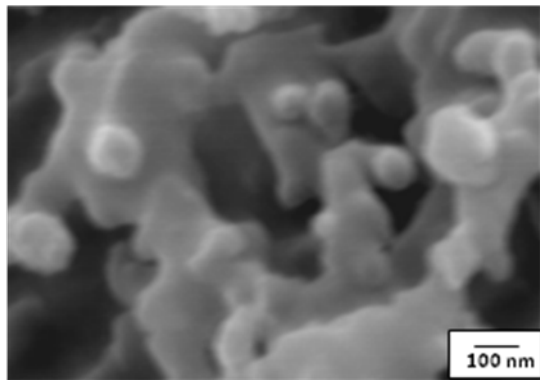
The particulates were trapped from exhaust gas from lamp and engine. The TEM method was used to visualize the particle diameter. The particulate size distribution in primary mode for approximately 100 particles which taken from TEM image, was shown in Fig. 6. Most of diesel lamp particle size is around 50-60 nm while the biodiesel lamp particle size has peaked in the range between 30-40 nm which is slightly smaller than that of diesel lamp particle. The peak of primary particle size from diesel and biodiesel engines are approximately 30-40 nm. The primary size of diesel particles is larger than that of biodiesel. This is due to the lower concentration of biodiesel particle, which is readily oxidized with more available oxygen in combustion flame due to oxygenated biodiesel fuel. On the other hand, the primary particle size from diesel engine is smaller than that of diesel lamp particle possibly because of engine conditions such as homogeneous of air/fuel mixture, high pressure in combustion chamber, exhaust gas temperature, may effect to particulate matter oxidation before exiting to the atmosphere. Moreover, higher oxygen content and homogeneity mixture closed to the stoichiometric condition of bio-oxygenated fuel can produce smaller size of primary particulate particle.



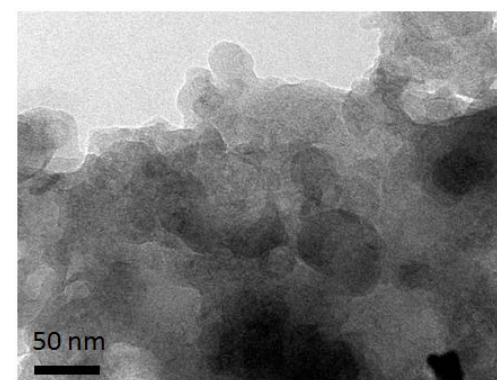
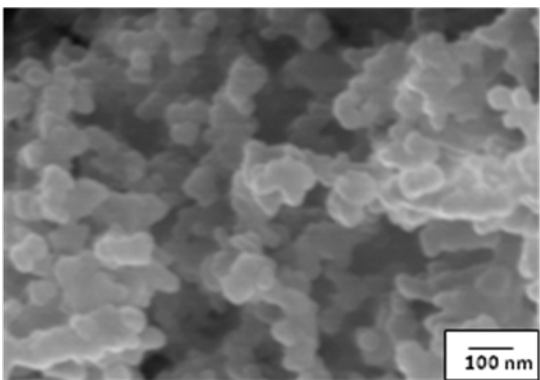
(a) SEM (left) and TEM (right) images of Diesel lamp PMs



(b) SEM (left) and TEM (right) images of biodiesel lamp PMs



(c) SEM (left) and TEM (right) images of diesel engine PMs



(d) SEM (left) and TEM (right) images of biodiesel engine PMs

Figure 5. SEM (left) and TEM (right) images of (a) Diesel lamp, (b) Biodiesel lamp (c) Diesel engine and (d) Biodiesel engine particulate matters [19-20]

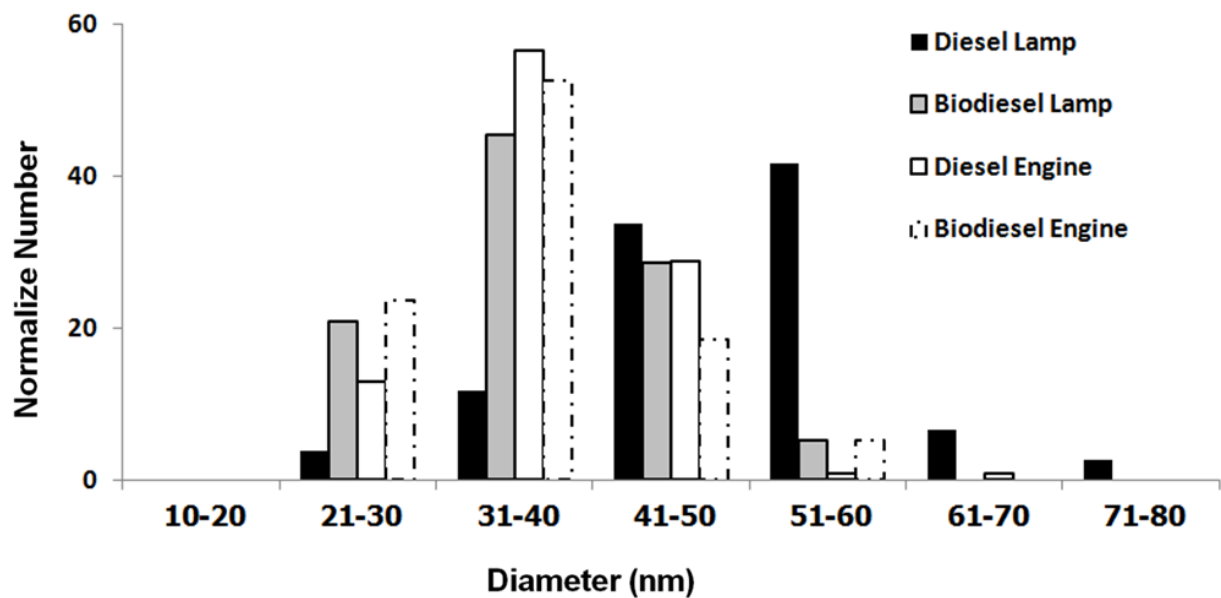


Figure 6. Primary particle size distribution of particulate matter by TEM images which normalized from 38 to 108 particles to be 100 samples of each fuel's particle

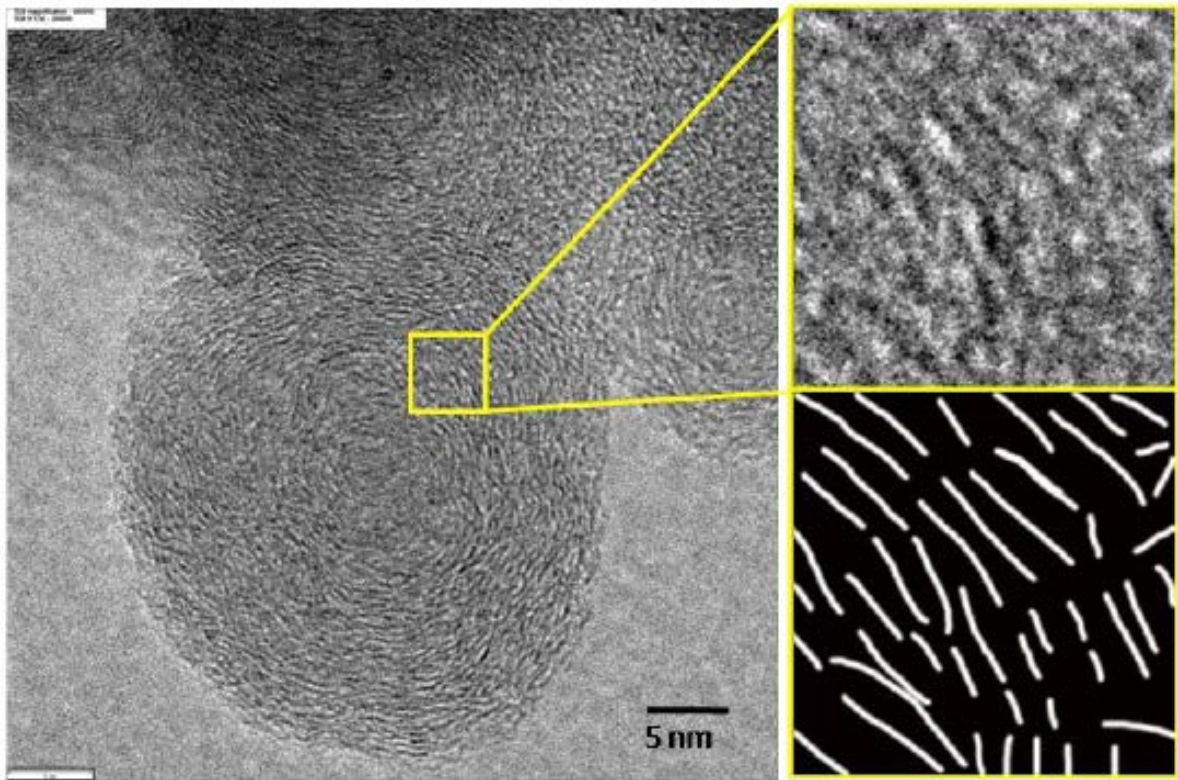
Nanostructure of Particulate Matter

Figure 7 shows the nanostructure of diesel particulate matter which emitted from diffusion flame combustion inside a diesel engine. Particulate matter is investigated for number of carbon atom contained in the particle. TEM image is used for numerating platelet number that aggregate layered in the particle. Each of platelets is consisted of proper amount of carbon atom from incomplete combustion product. For each of combustion, lamp and engine, the platelet sizes are shown in Fig. 8. The average of diesel and biodiesel carbon platelets is in the range of 0.5-3.0 nm. However the distance of each platelet for different fuels is not the same.

Another result of carbon atom number per volume is also estimated. The concept of estimation is "the molecule of carbon-6 (C6) is the possible smallest size". Such molecules are agglomerated to be the large ring of carbon then becomes a platelet. The particulate matter from biodiesel lamp and diesel lamp contain 129, 205 atom per nm^3 while the particulate matter from biodiesel engine and diesel engine are consisted by carbon atom number of 63 and 72 per nm^3 , respectively, as shown in Table 1.

The particulate matter from diesel combustion contains carbon atom that is larger than that of biodiesel combustion. The biodiesel combustion which emits lower carbon concentration results in lower carbon atom consisted in particulate matter. In addition, platelet length and atom concentration of particulate matter emitted from the engine are smaller than that of diffusion flame of lamp due to the impact of pressure, temperature and homogeneous mixture of fuel and oxygen.

This is an interesting result of bio-oxygenated fuel combustion behavior and particles emission nanostructure which should be researched in more details to discover the useful information for better understanding and future designs of modern Internal Combustion Engines and DPF configurations.



(a) TEM image

(b) Post process image

Figure 7. (a) TEM and (b) Post process (by hand draw) images of carbon platelet inside particulate matter

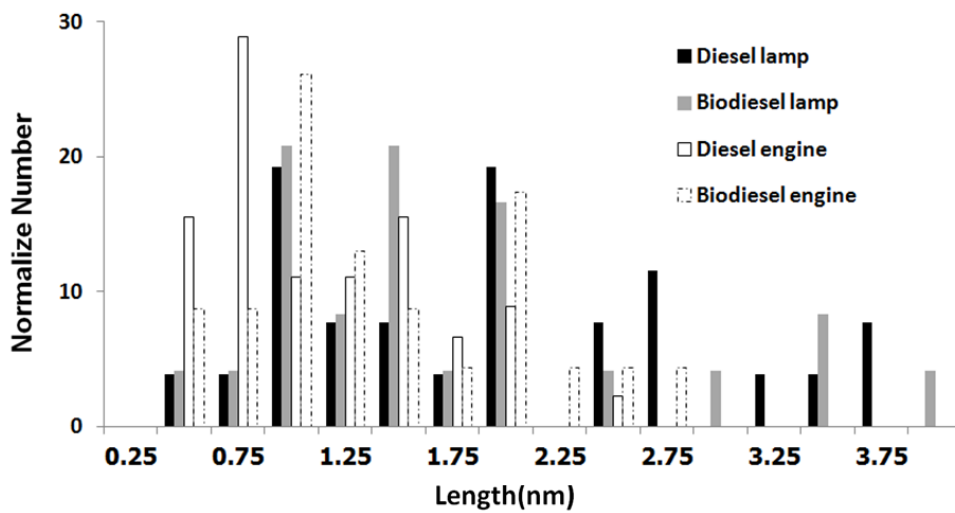


Figure 8. Carbon platelet size distribution of particulate matter by TEM images normalized from 24 to 45 platelets to be 100 samples of each fuel's particle

Table 1. Carbon Atom Include in Particulate Matter

Particulate Matter Type	Density (atom/nm ³)
Biodiesel Lamp PM	129
Diesel Lamp PM	205
Biodiesel Engine PM	63
Diesel Engine PM	72

Oxidation of Particulate Matter

Figure 9 (a) shows Arrhenius plots of diesel and biodiesel particulate matter oxidation by non-isothermal method of TGA at temperature of 400 °C to 480 °C using Eq.1-4. It is assumed that the diesel and oxygenate unburned hydrocarbons oxidation could be oxidized and calculated apparent activation energies are approximately 130 and 91 kJ/mol, respectively. On the other hand, temperature from 490 °C to 520 °C is assumed to be carbon oxidation which has 155-177 kJ/mol of apparent activation energy.

Figure 9 (b) shows Arrhenius plots of remaining pure carbon inside diesel and biodiesel particulate matter oxidation by TGA isothermal method at the temperature from 450 °C to 600 °C. Unburned hydrocarbons were assumed to be successfully oxidized before holding the constant temperature. Apparent activation energy of pure carbon is approximately 155 kJ/mol for both of diesel and biodiesel carbon.

Table 2 summarizes the apparent activation energy of each particulate matter oxidation by non-isothermal and isothermal methods. It is clearly observed that unburned bio-oxygenated hydrocarbon oxidized at the lower temperature and requires lower apparent activation energies than that of fossil fuel even the remaining carbon are oxidized in the same range of apparent activation energies.

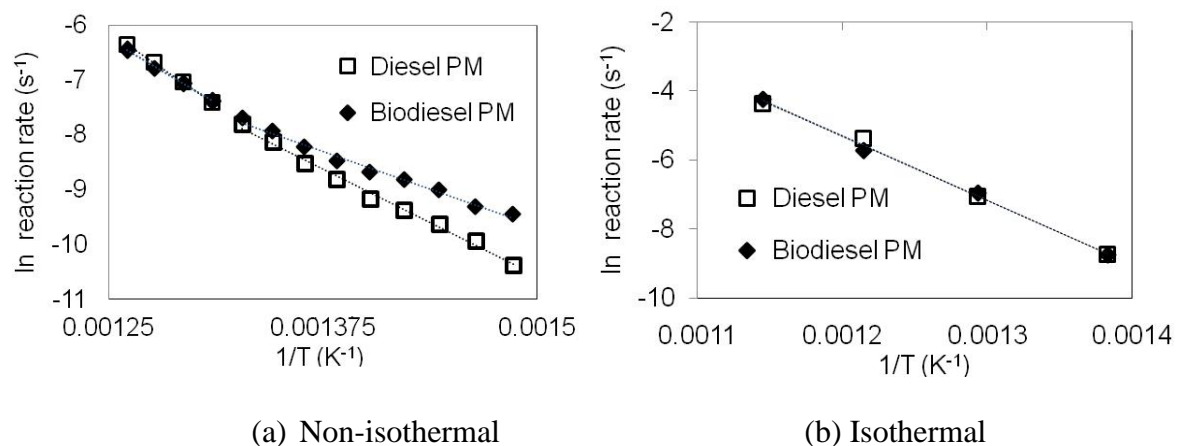


Figure. 9 Arrhenius plots of PM oxidation by (a) Non-isothermal and (b) Isothermal methods

Table 2. Apparent Activation Energy (Ea) of Particulate Matter Oxidation

Particulate Matter Type	Ea (kJ/mol)		
	Non-isothermal 400-480 °C	Non-isothermal 490-520 °C	Isothermal 450-600 °C
Biodiesel Lamp PM	91.3	155.4	155.6
Diesel Lamp PM	129.6	176.7	155.9

Conclusions

- Biodiesel combustion produces particulate matter two times lower than that of diesel combustion. Therefore, the conventional DPF can be used for two times of trapping duration. This means the energy consumption of engine for both the effect of pressure drop while driving and DPF regeneration process can be reduced approximately by two times.
- The primary size of diesel particles is larger than that of biodiesel. This is due to the lower concentration of biodiesel particles, which is readily oxidized with more available oxygen in combustion flame due to oxygenated biodiesel fuel. On the other hand, the primary particle size from diesel engine is smaller than that of diesel lamp particle due to homogeneous air/fuel mixture effect for complete combustion. However the impact is not strong for DPF trapping process because of the pore size of DPF is very large compared to the size of the particle emission.
- The carbon atom density in diesel particulate matter is higher than that of biodiesel. As a result, the impact of carbon and oxygen atom contents in oxygenated fuel must be researched for more understanding to optimize the internal combustion engine and DPF configurations.
- Unburned hydrocarbon from biodiesel combustion can be oxidized faster than that of unburned hydrocarbon from diesel combustion because of oxygen atoms included inside oxygenated fuel molecule promote complete combustion. Moreover, it is clearly observed that there is the same value of apparent activation energies for particulate matter without unburned hydrocarbon due to the condition of pure carbon oxidation.

References

- [1] J.B. Heywood, *Internal Combustion Engine Fundamental*, McGraw-Hill Education, Singapore, 1988.
- [2] O.I. Smith, "Fundamentals of soot formation in flames with application to diesel engine particulate emissions," *Progress in Energy and Combustion Science*, Vol. 7, pp. 275-291, 1981.
- [3] M.M. Maricq, "Review chemical characterization of particulate emissions from diesel engine: A review," *Journal of Aerosol Science*, Vol. 38, pp.1079-1118, 2007.
- [4] D.B. Kittelson, "Engines and nanoparticles: A review," *Journal of Aerosol Science*, Vol. 29, pp.575-588, 1998.
- [5] W.A. Majewski, and M.K. Khair, *Diesel Emissions and Their Control*, SAE International, Warrendale, United States, 2006.

- [6] T. Ishiguro, Y. Takatori, and K. Akihama, "Microstructure of diesel soot particles probed by electron microscopy: First observation of inner core and outer shell, *Combustion and Flame*, Vol. 108, pp. 231-234, 1997.
- [7] R.A. Vander Wal, A. Yezerets, N.W. Currier, D.H. Kim, and C.H. Wang, "HRTEM study of diesel soot collected from diesel particulate filters," *Carbon*, Vol. 45, pp. 70-77, 2007.
- [8] T. Aizawa, H. Nishigai, K. Kondo, T. Yamaguchi, J.G. Nerva, C. Genzale, S. Kook, and L. Pickett, "Transmission electron microscopy of soot particles directly sampled in diesel spray flame – A comparison between US#2 and biodiesel soot," *SAE International Journal of Fuels and Lubricants*, SAE International, Vol. 5, No. 2, pp. 665-673, 2012.
- [9] N. Miyamoto, H. Ogawa, and M.N. Nabi, "Approches to extremely low emissions and efficient diesel combustion with oxygenated fuels," *International Journal of Engine Research*, Vol. 1, No. 1, pp. 71-85, 2000.
- [10] A.G. Konstandopoulos, M. Kostoglou, N. Vlachos, and E. Kladopoulos, *Progress in Diesel Particulate Filter Simulation*, SAE Technical paper, 2005-01-0946, 2005.
- [11] A.G. Konstandopoulos, D. Zarvalis, E. Kladopoulou, and L. Dolios, *A Multi-Reactor Assembly for Screening of Diesel Particulate Filters*, SAE Technical paper, 2006-01-0874, 2006.
- [12] S. Tushima, I. Nakamura, S. Sakashita, S. Hirai, and D. Kitayama, *Lattice Boltzmann Simulation on Particle Transport and Captured Behaviors in a 3D-Reconstructed Micro Porous DPF*, SAE Technical paper, 2010-01-0534, 2010.
- [13] K. Hanamura, P. Karin, L. Cui, P. Rubio, T. Tsuruta, T. Tanaka, and T. Suzuki, "Micro- and macroscopic visualization of particulate matter trapping and regeneration processes in wall-flow diesel particulate filters," *International Journal of Engine Research*, Vol.10, No.5/2009, pp.305-321, 2009.
- [14] P. Karin, L. Cui, P. Rubio, T. Tsuruta, and K. Hanamura, "Microscopic visualization of PM trapping and regeneration in micro-structural pores of a DPF wall," *SAE International Journal of Fuels and Lubricants*, Vol. 2, No. 1, pp. 661-669, 2009.
- [15] P. Karin, and K. Hanamura, "Particulate matter trapping and oxidation on catalyst-membrane," *SAE International Journal of Fuels and Lubricants*, Vol. 3, No. 1 pp. 368-379, 2010.
- [16] H. Oki, P. Karin, and K. Hanamura, "Visualization of oxidation of soot nanoparticles trapped on a diesel particulate membrane filter," *SAE International Journal of Engines*, SAE International, Vol. 4, No. 1, pp. 515-526, 2011.
- [17] K. Nakamura, H. Oki, R. Sanui, and K. Hanamura, *Soot Oxidation Characteristics of SiC Nanoparticle Membrane Filters*, SAE Technical Paper, 2012-01-0848, 2012.
- [18] S. Laosuwan, P. Karin, and C. Charoenpornpanich, "Study on diesel and biodiesel particulate matter trapping inside a diesel particulate filter," Paper presented at *The 7th International Conference of Automotive Engineer (ICAE-7)*, TSAE, Bangkok, Thailand, March 28-29, 2011.
- [19] S. Laosuwan, P. Karin, and C. Charoenpornpanich, "Thermo-gravimetric analysis of biodiesel diffusion flame's particulate matter," Paper presented at *The Second TSME International Conference on Mechanical Engineering (The 2nd TSME-ICoME)*, Krabi, Thailand, October 19-21, 2011.
- [20] Y. Songsaengchan, C. Chareonphonphanich, P. Karin, N. Chollacoop, M. Thongroon, and K. Hanamura, "Physical characterization of biodiesel particulate matter by STEM," Paper presented at the *Second TSME International Conference on Mechanical Engineering (The 2nd TSME-ICoME)*, Krabi, Thailand, October 19-21, 2011.